

Influence of electronic correlations on orbital polarizations in the parent and doped iron pnictides

Ya-Min Quan¹, Liang-Jian Zou^{1,2*}, Da-Yong Liu¹, and Hai-Qing Lin²

¹ Key Laboratory of Materials Physics,
Institute of Solid State Physics, Chinese Academy of Sciences,
P. O. Box 1129, Hefei 230031, China

² Department of Physics, Chinese University of Hong Kong,
Shatin, New Territory, Hong Kong, China

(Dated: Nov 6, 2010)

Orbital polarization and electronic correlation are two essential aspects in understanding the normal state and superconducting properties of multiorbital FeAs-based superconductors. In this Letter, we present a systematical study on the orbital polarization of iron pnictides from weak to strong Coulomb correlations within the KRSB approach. The magnetic phase diagram of the two-orbital model for LaFeAsO clearly shows that the striped antiferromagnetic metallic phase with considerable orbital polarization exists over a wide doping range. The reversal of the orbital polarization occurs in the intermediate correlation regime. A small crystal field splitting enhances the orbital density wave order.

PACS numbers: 75.30.Fv, 74.20.-z, 71.10.-w

Since the discovery of high- T_c superconductivity (SC) in doped iron pnictides¹⁻³, the iron-based high- T_c SC material has been the subject of intensive researches in the past two years. Among various normal-state and SC properties of iron pnictides, the roles of the electronic correlation and the orbital polarization have been the central topics. The parent phases of cuprates are Heisenberg antiferromagnets (AFM) and insulators, and the important role of the electronic correlation and dominant single-orbital hole with the $x^2 - y^2$ symmetry were well established and verified. Unlike the high- T_c cuprates, the parent phase of iron pnictide SC are a bad metal², and usually exhibits spin-density-wave (SDW)-type or striped AFM ordering^{3,5}. What is the role of the electronic correlation and how many Fe 3d orbitals are involved in the iron pnictides are two essential and key aspects to understand various properties in the SDW metallic and SC phase.

Up to date, experimental evidences on the role of electronic correlation in parent phase and SC phases are controversial. Indeed, the metallic conductivity^{1,2}, small magnetic moment of Fe spins⁵, X-ray absorption spectroscopy (XAS) and resonant inelastic X-ray scattering (RIXS) of Fe⁴ in undoped iron pnictides seem to suggest a weak correlation between Fe 3d electrons. From the resonant X-ray emission spectroscopy (RXES) of Fe 3d $L_{2,3}$ edges, Kurmaev et al.⁶ suggested that the 111 phase is a weakly or at most moderately correlated system. However, many more experimental clues demonstrated the band narrowing effect, suggesting the important roles of the 3d electronic correlation^{4,6,7}. In fact, in addition to the band narrowing effect, the existence of intermediate magnetic moment in the 1111, 122 and 111 phases also shows the importance of the electronic correlation. Therefore one should employ an approach applicable for both weak and strong Coulomb interactions so as to uncover the roles of electronic correlations on the electronic states and magnetic

configuration in iron pnictides.

On the other hand, it is still under hot debate in literature on how many orbitals are involved and what the orbital symmetry of the bands near E_F is in the parent and doped iron pnictides. Theoretically, two-orbital⁸, three-orbital⁹, four-orbital¹⁰ and even five-orbital^{11,12} tight-binding model were proposed. Most of the multi-orbital tight-binding models captured the major Fermi surface and dominant band structure characters near E_F of the 1111 and 122 phases. To distinguish the validity of these models is essential to reveal the symmetry character and the number of the orbitals involved in various iron pnictides.

The role of the electronic correlation in the groundstate properties of parent iron pnictides was discussed in very recent papers^{14,15}. To uncover the roles of the electronic correlation and orbital polarization in high- T_c iron pnictide SC, we apply the Kotliar-Ruckenstein's slave boson (KRSB) method¹³ on the two-orbital Hubbard models. The KRSB approach and its extension may provide a useful tool to treat the multi-orbital Hubbard model over a wide correlation range. It also has a few advantages in dealing with multiple orbitals, nontrivial magnetic configurations and spatial correlations. Our recent numerical ansatz developed for the multi-orbital KRSB solution overcomes the convergency of many parameters in minimizing the groundstate energy, suitable for treating arbitrary coulomb interaction in the presence of interorbital hoppings or hybridizations and various magnetic configurations.

In this paper, we first present the magnetic phase diagram of two-orbital model and demonstrate that in the intermediate electronic correlation, the striped AFM (SAFM) phase with small magnetic moment is stable against the paramagnetic (PM), ferromagnetic (FM) and Néel AFM phases, accompanied with a small orbital polarization, or a ferro-orbital density wave (F-ODW) order. A small crystal field splitting arising from the lattice distortion further stabilizes the SAFM and F-ODW ground state. The evolution of the orbital occupation and Fermi surface with the electron correlation shows that the

*Correspondence author, Electronic mail: zou@theory.issp.ac.cn

contribution of the d_{xz} orbital symmetry is larger than that of the d_{yz} orbital. These results clearly show the importance of the intermediate electronic correlation in the parent and doped phases of iron pnictides.

We start with two-orbital model Hamiltonian $H = H_0 + H_I$ applied for iron pnictides in real space with

$$H_0 = - \sum_{\langle ij \rangle \alpha \beta \sigma} (t_{\alpha\beta} c_{i\alpha\sigma}^\dagger c_{j\beta\sigma} + h.c.) + \sum_{i\alpha\sigma} (\varepsilon_\alpha - \mu) n_{i\alpha\sigma} \quad (1)$$

$$H_I = U \sum_{i\alpha} n_{i\alpha\uparrow} n_{i\alpha\downarrow} + \sum_{i\sigma\sigma'(\alpha>\beta)} (U' - J_H \delta_{\sigma\sigma'}) n_{i\alpha\sigma} n_{i\beta\sigma'} - J_H \sum_{i\alpha\neq\beta} (c_{i\alpha\uparrow}^\dagger c_{i\alpha\downarrow} c_{i\beta\downarrow}^\dagger c_{i\beta\uparrow} - c_{i\alpha\uparrow}^\dagger c_{i\alpha\downarrow}^\dagger c_{i\beta\downarrow} c_{i\beta\uparrow}), \quad (2)$$

where $C_{i\alpha\sigma}^\dagger$ creates an electron with orbital index α and spin σ at lattice site i , $n_{i\alpha\sigma}$ is the corresponding occupation number operator. The hopping integral for the orbital α and β is denoted by $t_{\alpha\beta}$. The intraband (inter-band) Coulomb repulsion and Hund's rule coupling are denoted by U (U') and J_H , respectively. Here we set $U' = U - 2J_H$.

To reflect the multi-orbital character of iron pnictides, we extend the single-orbital KRSB approach¹³ to the two-orbital Hubbard models for various magnetic configurations. In the multiorbital Hubbard model, a few of auxiliary boson field operators representing the possibilities of various electron occupations are introduced, such as e, p, d, b, t, q , which denote the possibilities of none, single, double, triplicate, quaternary occupations. With these auxiliary boson fields, an original fermion operator can be expressed as:

$$c_{i\alpha\sigma}^\dagger = Q_{i\alpha\sigma}^{-\frac{1}{2}} \left(p_{i\alpha\sigma}^\dagger e_i + b_{i\alpha}^\dagger p_{i\alpha\sigma} + \sum_{\sigma'} d_{i\sigma\alpha\sigma'}^\dagger p_{i\beta\sigma'} + t_{i\alpha\sigma}^\dagger b_{i\beta} \right) + \sum_{\sigma'} t_{i\beta\sigma'}^\dagger d_{i\bar{\sigma}\alpha\sigma'} + q_i^\dagger t_{i\alpha\bar{\sigma}} \left(1 - Q_{i\alpha\sigma} \right)^{-\frac{1}{2}} f_{i\alpha\sigma}^\dagger \quad (3)$$

Here $f_{i\alpha\sigma}^\dagger$ is the new slaved fermion operator and $Q_{i\alpha\sigma}$ is an auxiliary particle number operator¹³. Projecting the original fermion operators into these boson field and fermion field operators, one could not only obtain an effective Hamiltonian, but also get the groundstate energy in the saddle point approximation with the normalization condition and the fermion number constraints¹³. Here we employ a generalized Lagrange multiplier method to enforce these constraint conditions, thus the interorbital hoppings and crystal field splitting can be treated on the same foot. The fermion occupation number is constrained with the penalty function method. To enforce the normalization condition, we have a boundary constrained condition:

$$1 \geq \sum_{\alpha\sigma} p_{\alpha\sigma}^2 + \sum_{\alpha} b_{\alpha}^2 + \sum_{\alpha\sigma\sigma'} d_{\alpha\sigma\sigma'}^2 + \sum_{\alpha\sigma} t_{\alpha\sigma}^2 + q^2 \quad (4)$$

We use optimizing method to get the minimized groundstate energy. To search for possible ground state, we study four different magnetic configurations, including the PM or nonmagnetic, FM, *Néel* AFM and SAFM phases so as to find the stable ground state.

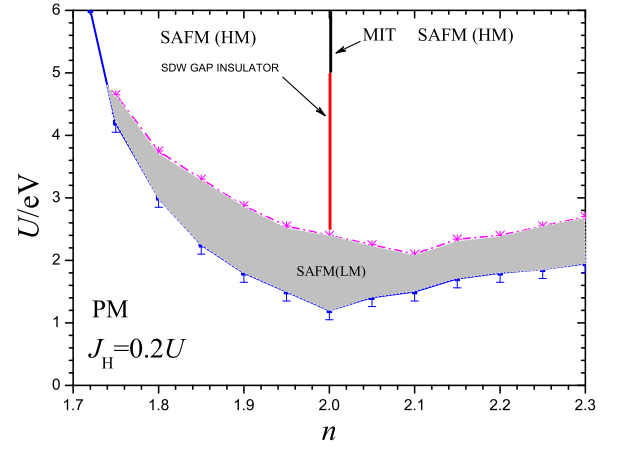


FIG. 1: Magnetic phase diagram as a function of particle density n and correlated U for $J_H = 0.2U$. PM, SAFM(LM) and SAFM(HM) stand for paramagnetic metallic, striped antiferromagnetic metallic phases with magnetic moment $m < 1\mu_B$ and $m > 1\mu_B$, respectively.

As the penalty factor is sufficiently large, the particle number constraint is satisfied. Nevertheless, the problem of boundary constrained condition is still difficult. In numerically searching the global minima of the groundstate energy, we employ the pattern search method, together with the gradient method and the Rosenbrock method. If the optimizing point is on the boundary, we move one step inward the high-dimensional ellipsoid and the equipotential plane. Since the first axis of the new local orthogonal coordinate system of Rosenbrock method directs to the negative gradient direction, the corresponding algorithm is simple. To investigate the groundstate electronic and magnetic properties of iron pnictides, we adopt the hopping parameters of Zhang *et al.*⁸ for the two-orbital situation in the present slave boson scheme. In the two-orbital situation, the orbits 1 and 2 refer to the d_{xz} and d_{yz} components, respectively.

We first obtain the magnetic-phase diagram of the two-orbital system through comparing the energies of the PM (or nonmagnetic), FM, *Néel* AFM and SAFM configurations. In the present symmetric orbital situation, the penalty factors adopted for the two degenerate orbits are identical. This will save a great deal of computation time in minimizing the total energy.

Fig.1 displays the zero-temperature phase diagram of U vs n for Zhang *et al.*'s⁸ hopping parameters. We consider the full Hund's coupling J_H , which equals to $0.2U$. One notices that only the PM metallic phase is stable when the on-site Coulomb correlation $U < U_{c1} \approx 1.2$ eV. When $U > U_{c1}$, the SAFM phases are stable over wide doping and interaction ranges. This SAFM region can be divided into high magnetic moment one (SAFM(HM)) with $m > 1\mu_B$ and low magnetic moment one (SAFM(LM)) with $m < 1\mu_B$. The latter lying in $U_{c1} < U < U_{c2}$ is the most interesting and marked with a shadow since the magnetic moments of the parent and doped phases of the most of iron pnictides, including the 1111, 122 and 111 phases, fall into this region. In the present phase diagram, it is also shown that the SAFM(LM) regime is limited

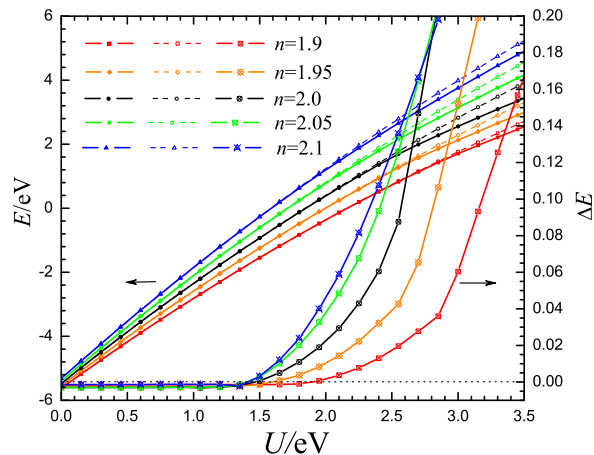


FIG. 2: Electronic correlation dependence of total energies of PM phase (dashed line) and SAFM phase (solid line) and that of the energy difference ($E_{PM} - E_{SAFM}$) between these two magnetic configurations at $n = 1.9, 1.95, 2, 2.05$ and 2.10 , respectively.

to a very narrow range.

Especially interest is found around the particle filling number of $n = 2$. One notices that the phase diagram is not symmetrical about the half filling ($n = 2$) due to the presence of the next nearest-neighbor hopping. When $U > U_{c1}$, the system enters the spin gapped insulating phase. In this insulating region the gap between the spin-down and spin-up subbands, the sublattice magnetic moment, the spin exchange splitting and the quasiparticle bandwidth increase with the increase of U . When the electronic correlation becomes so strong that $U > 5$ eV, the system enters a full gapped region, very similar to the conventional Mott insulating phase. In the insulating region, with the further increase of the Coulomb interaction U , the spin exchange splitting approaches a constant and sublattice magnetic moment is saturated. In comparison with the conventional PM Mott phase, the quasiparticle bandwidth in this SAFM Mott phase gradually decrease with the increase of U again. As shown in the following, the orbital polarization is observed in a wide doping and an interaction regime, while no orbital polarization is seen at $n = 2$ when the correlation is strong.

For more clarity, we plot the correlation dependence of the groundstate energies in the PM structure and the SAFM one in Fig.2. Also an energy difference, $E_{PM} - E_{SAFM}$, between these two phases is displayed. One finds that when the electronic correlation is weak, or $U < U_{c1}$, the energy difference is negative and very small. So the PM phase is stable against the SAFM one. When the correlation reaches to the intermediate strength that $U > U_{c1}$, the energy difference becomes positive, the SAFM phase becomes more stable than the PM phase. Furthermore, one could estimate the magnitude of the magnetic couplings between iron spins. The magnetic coupling strength crucially depends on the doping concentration and electron correlations, as seen in Fig.2. For a typical parent compound LaOFeAs, the on-site Coulomb correlation between Fe $3d$ electrons is estimated to $2 \sim 3$ eV²¹. This gives rise to the magnetic coupling strength about 20 meV

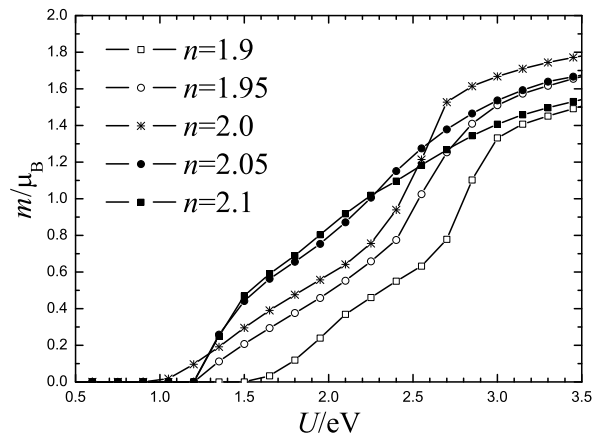


FIG. 3: Sublattice magnetic moment in the SAFM phase as a function of the Coulomb repulsion strength U . Theoretical parameters are the same to Fig.1.

at $n = 2$, in the same magnitude order of the spin coupling between Fe ions in LaOFeAs deduced from the neutron scattering experiment⁵.

Fig.3 shows the evolution of sublattice magnetic moments with the increase of the electronic correlation in the SAFM phase. It shows that the system remains PM without any magnetic ordering unless U becomes larger than U_{c1} , which increases with hole doping. In the realistic parameter range, *i.e.*, intermediate correlation regime, the magnetization decreases with the increase of hole doping, in agreement with the experiment observation. We notice that the minimal value of U_{c1} is about 1.2 eV at $n = 2$, which is considerably larger than the mean-field approximation results for the two-orbital model^{17,18}. It is also found that the sublattice magnetic moment increases continuously until U reaches $U_{c2} = 2.4$ eV, where it changes discontinuously. This behavior is also found by Yu *et al.* in the mean-field solution in the four-orbital model¹⁷. Further, the upper critical value for the SAFM regime with $m < 1\mu_B$ is 2.4 eV for $n = 2.0$, significantly larger than that obtained by the mean-field approximation^{17,18}, suggesting that the quantum fluctuations are well considered within the present KRSB approach. At $n = 2.0$, the sublattice magnetic moment is larger than $1\mu_B$ when $U > U_{c2} = 2.4$ eV. The SAFM system enters the high magnetic moment region, this is also shown in Fig.1. By monitoring the density of states (DOS) near the Fermi surface, we find that due to strong correlation, the system becomes insulating at $n = 2.0$. We notice such a fact that when the systems cross over from the SAFM insulating phase to the full-gap Mott one, the sublattice magnetic moments of the systems with $n = 1.9$ and 2.1 , or $n = 1.95$ and 2.05 , approach the same values, as seen in Fig.3, showing that the electron-hole symmetry restores in the strong correlation regime.

In the present two-orbital model, we can address the orbital polarization or orbital ordering problem in the parent and doped phases of LaOFeAs. We find that in the weakly correlated PM phase, due to the equivalence of the present two orbitals, the symmetry of two orbitals is not broken, no

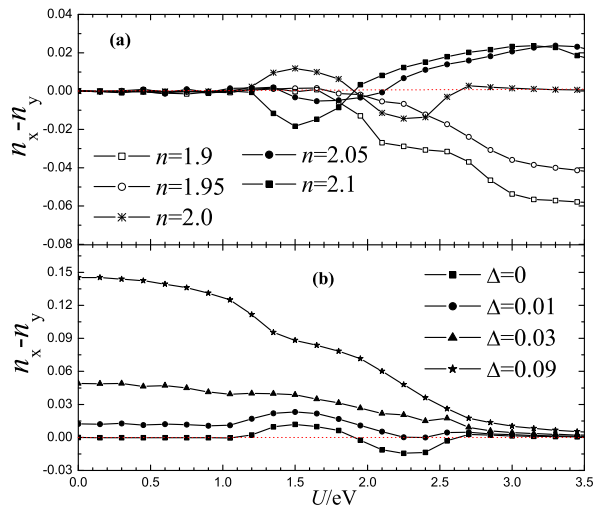


FIG. 4: Magnetic and crystal field dependence of orbital polarizations or itinerant orbital density wave ordering in two-orbital models. Theoretical parameters are the same to Fig.1.

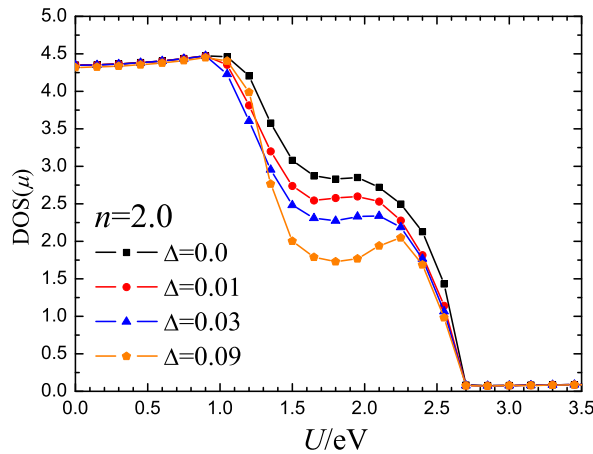


FIG. 5: The DOS at the Fermi surface as a function of U at different doping concentrations.

orbital polarization or orbital ordering is observed. As soon as the system enters the intermediate correlated SAFM phase, the orbital polarization is observed, as seen in Fig.4. Fig.4(a) shows that in the SAFM phase, the orbital polarization considerably depends on the Coulomb correlation and particle filling. When $n < 2$, the orbital polarization is negative, or the d_{yz} component is enhanced with the increase of U . At $n = 2$, the orbital polarization only occurs in the intermediate corre-

lation regime, and the polarization is reversed at $U_o = 1.9$ eV; when $U_{c1} < U < U_o$ the polarization is dominated by the d_{xz} component, while it is dominated by the d_{yz} component when $U_o < U < U_{c2}$. When $U > U_{c2}$, due to strong correlation, the two electrons occupy two orbitals with the same possibility, giving rise to a vanishing polarization. This behavior was also found in the conventional mean-field approximation¹⁹. When $n > 2$, we notice that the polarization also reverses the sign at about U_o . Though such an orbital polarization of ordering is weak, it is greatly enhanced in the presence of a small crystal field splitting, as shown in Fig.4(b). From Fig.4(b) one finds that the orbital polarization do not reverse over a wide correlation regime in the presence of crystal field splitting, while a kink at $U = 0$ still exists for various splitting.

These results clearly demonstrate that the orbital polarization or ferro-orbital ordering is accompanied with the onset of the SAFM ordering in the intermediate correlated iron pnictides. Since in the intermediate correlation regime, the system is metallic, a question naturally arises that what the essential of the F-ODW ordering is in metallic iron pnictides. Obviously, such an orbital polarization is essentially itinerant, as the itinerant FM in transition metals. Hence the orbital ordering in iron pnictides is characteristic of density wave. As we pointed out in an early paper²⁰, such an itinerant ferro-orbital ordering can occur as soon as a Stoner-like condition is satisfied²⁰. Besides, in Fig.5, we also display the correlation dependence of the quasiparticle DOS near E_F in the present two-orbital systems. It is found that the DOS increases slowly in the weak correlated PM region. With the increase of U , the DOS first steeply decreases and then slightly increases in the metallic SAFM ordered phase with small magnetic moment, demonstrating a pseudogap behavior. The pseudogap in the intermediate correlation regime turns to a full gap in the spin-density-wave gap insulating phase when $U > 2.7$ eV. From the analysis on the spin-dependent partial DOS, we find this full gap is triggered by spin polarization. When $U > 4.1$ eV, the system enters a conventional Mott insulator phase.

In summary, we have shown that in the parent and doped phases of iron pnictides, the intermediate electronic correlation favors a striped antiferromagnetic configuration accompanied with a small structural distortion and weak ferro-orbital ordering. The orbital polarization is the characteristics of a ferro-orbital density wave.

This work was supported by the NSFC of China No.10874186, 11074257 and 11047154. Numerical calculations were performed at the Center for Computational Science of CASHIPS.

¹ Y. Kamihara, *et al.*, J. Am. Chem. Soc. **130**, 3296 (2008).

² X. H. Chen, *et al.*, Nature London **453**, 761 (2008).

³ G. F. Chen, *et al.*, Phys. Rev. Lett. **100**, 247002 (2008).

⁴ W. L. Yang, *et al.*, Phys. Rev. B. **80**, 014508 (2009).

⁵ S. J. Zhang, *et al.*, Phys. Rev. B. **80**, 014506 (2009).

⁶ E. Z. Kurmaev, *et al.*, J. Phys. Condens. Matter. **21**, 345701 (2009).

⁷ H. Ding *et al.*, arXiv:0812.0534..

⁸ S. Raghu, *et al.* Phys. Rev. B **77**, 220503(R) (2008).

⁹ P. A. Lee and X. G. Wen, Phys. Rev. B **78**, 144517(R) (2008).

¹⁰ M.M. Korshunov, and I. Eremin, Phys. Rev. B **78**, 140509(R) (2008).

¹¹ K. Haule, J. H. Shim and G. Kotliar, Phys. Rev. Lett. **100**, 226402

- (2008).
- ¹² K. Kuroki, S. Onari, R. Arita, H. Usui, Y. Tanaka, H. Kontani, and H. Aoki, Phys. Rev. Lett. **101**, 087004 (2008).
- ¹³ G. Kotliar and A. Ruckenstein, Phys. Rev. Lett. **57**, 1362 (1986)
- ¹⁴ S. Zhou and Z. Q. Wang, Phys. Rev. Lett. **105**, 096401 (2010).
- ¹⁵ W.-H. Ko and P. A. Lee, arXiv:1101.5183.
- ¹⁶ H. Hasegawa, Phys. Rev. B **56**, 1196 (1997)
- ¹⁷ Rong Yu, *et al.*, Phys. Rev. B **79**, 104510 (2009)
- ¹⁸ Maria Daghofer, *et al.*, Phys. Rev. B **81**, 014511 (2010)
- ¹⁹ M. Daghofer, *et al.*, Phys. Rev. B **81**, 180514 (2010)
- ²⁰ Feng LU, *et al.*, Chin. Phys. Lett. **26**, 097501 (2009)
- ²¹ V. I. Anisimov, *et al.* J. Phys.: Condens. Matter **21** 075602 (2009).